257671

AD No. 257671
ASTIA FILE COPY

61-3-4
XEROX

(1)

MCL - 476/1

TECHNICAL DOCUMENTS LIAISON OFFICE
UNEDITED ROUGH DRAFT TRANSLATION

CERTAIN PROPERTIES OF BORIDE ALLOYS OF REFRACTORY TRANSITION METALS

BY: G. A. Meyerson, et. al.

English Pages: 26

SOURCE: Konferentsiya Po Khimii Bora I Yego Soyedinenii, 1955, pp. 58-73.

$2.60

17575

THIS TRANSLATION HAS BEEN PREPARED IN THIS MANNER TO PROVIDE THE REQUESTER WITH INFORMATION IN THE SHORTEST POSSIBLE TIME. FURTHER EDITING WILL NOT BE ACCOMPLISHED BY THE PREPARING AGENCY UNLESS FULLY DETAILED IN WRITING TO THE CHIEF, TECHNICAL DOCUMENTS LIAISON OFFICE, MCLTD, WPAFB, OHIO

PREPARED BY:

TECHNICAL DOCUMENTS LIAISON OFFICE, MCLTD
WPAFB, OHIO

MCL - 476/1

Date 1 Nov. 1960

MCL-476/1

CERTAIN PROPERTIES OF BORIDE ALLOYS OF REFRACTORY TRANSITION METALS

(NEKOTORYYE SVOYSTVA SPLAVOV BORIDOV TUGOPLAVKIKH PEREKHODNYKH METALLOV)

G. A. Meyerson, G. V. Samsonov, R. B. Kotel'nikov, M. S. Voynova, I. F. Evteyeva and Z. D. Krasnenkova

(Institute of Nonferrous Metals and Gold of Moscow)

M. I. Kalinin

In the aviation, metallurgical, and chemical industries as well as in other fields of technology, there is a need for materials possessing a high degree of corrosion and heat resistance, chemical stability, special electrical properties, hardness, etc. Such materials, in particular, are the compounds of refractory, transition metals with light metalloids such as nitrides, carbides, borides, silicides and others. In this connection, studies of the properties of such compounds have recently been expanded.

Great attention is being payed to the study of borides, which until recently were studied less than the carbides and nitrides.

In hardness and corrosion resistance borides surpass carbides and also possess comparatively small density, and are good conductors of heat and electricity, etc.

The fields in which borides of refractory, transition metals can be applied are quite varied. In the literature there are reports of their use in the production of hard alloys for making gas turbine parts, in the manufacture of nozzles for metallized equipment, exhaust pipes for engines, centrifuge parts, pistons for automatic presses, crucibles for fusion of refractory metals, protective pipes for thermocouple immersion pyrometers, etc. [1 through 4].

Borides of refractory transition metals are also of interest from the view point of the theory of the structure of metal compounds. The uniqueness of borides lies in the fact that by possessing a number of characteristics which are typical of the so-called "interstitial phases", they do not have the ordinary "interstitial" structure due to the large size of the boron atom.

The boride alloys are of significant practical and theoretical interest, despite the fact that their study is in the beginning stage.

In the present work, TiB_2 - CrB_2, TiB_2 - W_2B_5, and ZrB_2 - Cr_3B_2 systems were studied. After taking into account the properties of the initial borides and the possible technical use of their alloys, the research was conducted along the following basic lines:

(1) The study of the phase composition and structures of the products of the diffusion reaction of the initial borides;

(2) The study of the microhardness of the phases; and

(3) The study of the corrosion resistance and the structure of scales of various compositions.

Alloys TiB_2 - CrB_2 and ZrB_2 - CrB_2 were interesting from the viewpoint of the combination of two borides, each having high corrosion resistance. Moreover, chromium boride (CrB_2) is the least expensive of the refractory, hard borides.

borides and, if only for that reason, alloys on this base deserve more serious study.

Comparison of these systems also had a certain interest from the view point of experimentally checking the conditions of the formation of a continuous series of solid solutions [5].

The system $TiB_2 - W_2B_5$ is analogous to the carbide system TiC - WC, which found wide application in the production of hard alloys, and thus it was possible in the present case to expect a certain increase in the microhardness of the phases.

The literature contains a number of indications regarding the existence of titanium boride Ti_2B_5, which is isomorphic with the tungsten boride W_2B_5. On this basis it was possible to presume the existence of considerable solubility of titanium boride in W_2B_5, due to the transformation of the structure of TiB_2 into TiB_5 (similar to tungsten carbide alloys having a hexagonal structure alloyed with carbides with a cubic lattice [7, 8]).

Obtaining Borides

Starting powdered borides TiB_2, ZrB_2, CrB_2, W_2B_5 were obtained by a vacuum-thermal method from their respective metal oxides (TiO_2, ZrO_2, Cr_2O_3 and WO_3), boron carbides and calcined soot, in the laboratory vacuum resistance furnace of a retort type with a graphite heater [10]. The calcination methods are given in Table 1.

The obtained borides were ground in a ball mill, in a water medium, and the iron impurities washed out by diluted acid.

Table 2 shows the results of a chemical, x-ray diffraction, and granulometric analysis of these borides.

3

As seen from Table 2, the chemical composition of powdered borides is nearly stoichiometric, and the spacing of the crystal lattices, determined within the limits of accuracy of the study, corresponds to data in the literature. The density determined by the micropycnometric method [11] agrees with the density calculated from x-ray diffraction data.

TABLE 1

Method of Obtaining Borides

Method indices	TiB_2	ZrB_2	CrB_2	W_2B_5
Temperature, °C	1540	1770	1670	1340
Soaking, min	60	60	60	30
Content of soot in the furnace charge as % of the calculated quantity	100	95	95	90

TABLE 2

Characteristics of Powdered Borides

Indices	TiB_2	ZrB_2	CrB_2	W_2B_5
Metal content, % found	69.4	80.2	70.1	90.7
stoichiometric	68.9	80.8	70.6	89.2 *
Boron content, % found	30.6	19.3	29.9	9.8
stoichiometric	31.1	19.2	29.4	10.8 *
Carbon content, % C (total)	0.7	0.1	0.05	0.9
Iron content, %	1.0	0.8	0.4	2.0
Density, g/cm^3				
found	4.52	6.09	5.22	11.0
calculated	4.52	6.15	5.26	13.0
mean grain size, μ	2.0	4.0	2.6	4.6
Lattice spacing, kX μ				
a				
found	3.015±0.004	3.150±0.006	2.966±0.011	2.96±0.01
from literary data	3.022±0.002	3.163±0.002	2.963	2.976
c				
found	3.216±0.015	3.503±0.006	3.062±0.015	13.8±0.1
from published data	3.222±0.002	3.543±0.002	3.060	13.83
c/a				
found	1.066	1.114	1.035	4.66
from published data	1.066	1.114	1.033	4.76

* According to Kiessling [10] A_xB_y has a defective lattice, and the actual composition of the product corresponds to formula $B_{...}$. The composition for $B_{...}$ is given.

Obtaining and Investigating Alloys

Compact samples of alloys were obtained from mixtures of powdered borides by the method of hot pressing in graphite molds on the laboratory press with a lever mechanism for loading. A series of samples were prepared, differing by 10% mole of each component (and with 5% W_2B_5 for alloys TiB_2 - W_2B_5). The samples for the metallographic study, for determination of the compressive strength and for the study of oxidation processes, were 14 mm in diameter and about 4 mm in height. To determine the electrical conductivity and the coefficient of linear expansion, samples 8 mm in diameter and 15 to 20 mm in height were prepared. The porosity of the samples did not exceed 2 - 3%. The optimum temperature for hot pressing the borides was (in °C):

TiB_2	2500	CrB_2	2130
ZrB_2	2500	W_2B_5	2370

Above these temperatures, the samples melted, losing their metallic luster and turning black. This was evidently due to the reaction of the borides with the carbon of the dies and with the formation of comparatively low-melting eutectics.

The metallographic study was made on sections prepared in the usual way. In order to expose the structure, sections of alloys TiB_2 - CrB_2 were treated with a mixture of HF + HNO_3 + glycerine (1 : 1 : 1), sections of alloy ZrB_2 - CrB_2 with a mixture of HF + HNO_3 (1 : 1), and sections of TiB_2 - W_2B_5 by a mixture of HCL + HNO_3 (1 : 1), or a concentrated solution of Na_2SiFe in HNO_3.

Alloys TiB_2 - CrB_2 in the entire range of compositions had a single-phase structure. The structure of alloys TiB_2 - W_2B_5 and ZrB_2 - CrB_2 is a two-phase structure.

Fig. 1 shows the dependence of the mean grain size of alloys CrB_2—TiB_2 and CrB_2 - ZrB_2 on the composition. As seen from this Fig., the dependence curve of the grain size on the alloy composition of TiB_2 - CrB_2 has a clearly expressed maximum in the region of high chromium-boride content. The increase in grain size of alloys TiB_2 - CrB_2 with an increase in CrB_2 content is evidently explained by the lower melting temperature of chromium boride. Therefore the annealing of alloys rich in chromium boride occurred at a comparatively higher temperature, and the conditions for the growth of the grains were more favorable. The considerable decrease in the grain size during transition to the pure chromium boride can probably be explained by the nearness of the annealing temperature to the melting point. Under these conditions recrystallization occurred simultaneously around a great number of nuclei, thereby causing a decrease in grain size. A similar phenomenon was observed when, during the annealing of tungsten, the temperature approached the melting point.

X-ray diffraction studies were made by the powder method of taking x-ray photographs with copper radiation. As shown in Fig. 2, Vegard's law is closely observed for alloys TiB_2 - $Cr3_2$; within the limits of accuracy of our measurements, the points lay on straight lines. The variation in the spacings of the lattice components in alloys TiB_2 - A_2B_5 and ZrB_2 - CrB_2 is negligible and is within the accuracy of the measurements.

The electrical conductivity of alloys TiB_2 - $Cr3_2$ and ZrB_2 - CrB_2 was measured by the Thompson bridge. Cylindrical samples had an 8 mm diameter and a length of about 20 mm ; their porosity fluctuated between 5 and 10%. The resistivity values were reduced to zero porosity by the formula

$$\rho \text{ comp.} = \rho \text{ por.} (1-\Pi)$$

where ρ is the resistivity of the compact (ρ comp.) and porous (ρ por.) material;

Π is the porosity in fractions of one.

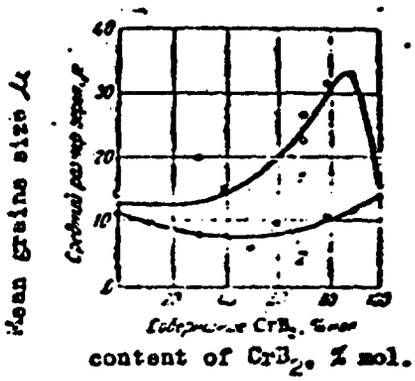

Fig. 1. Dependence of mean grain size of alloys of chromium diboride with diborides of titanium and zirconium on their composition (after annealing at 2000° for four hours):
(1) alloy CrB_2 - TiB_2 (2) alloy CrB_2 - ZrB_2

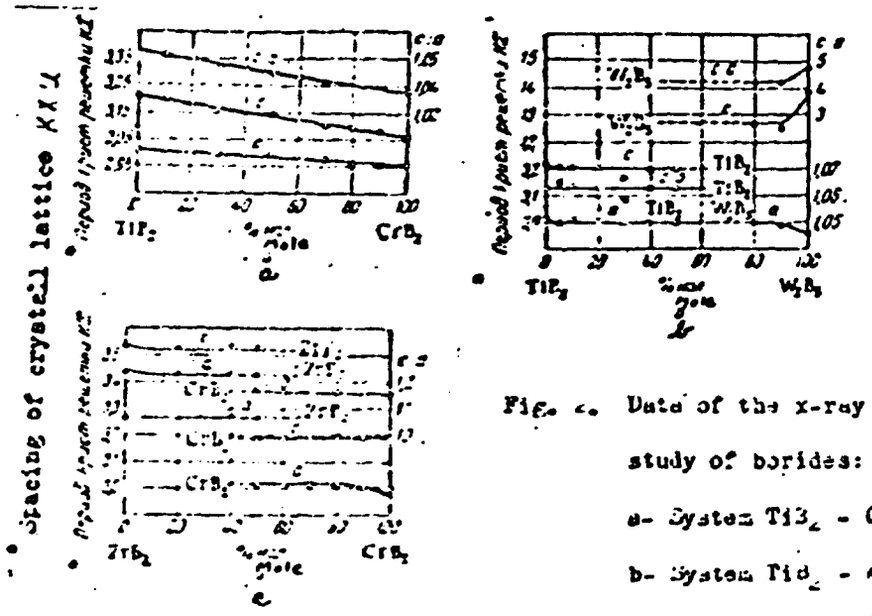

Fig. 2. Data of the x-ray diffraction study of borides:
a- System TiB_2 - CrB_2
b- System TiB_2 - W_2B_5
c- System ZrB_2 - CrB_2

..The position of the maximums of electrical conductivity and microhardness on the "composition-property" curves coincides in the first approximation (Fig. 3).

The microhardness of the phases was measured on etched sections with a PMT-3 instrument under a load of 30 g. As seen in Fig. 3 for alloys TiB_2 - CrB_2, the curve of the dependence of microhardness on the composition is smooth, with a maximum of 4200 kg/mm^2 at 80% mole TiB_2. Corresponding microhardness curves of phases of alloys TiB_2 - Ta_2B_5 and ZrB_2 - CrB_2 have a form characteristic of two-phase alloys.

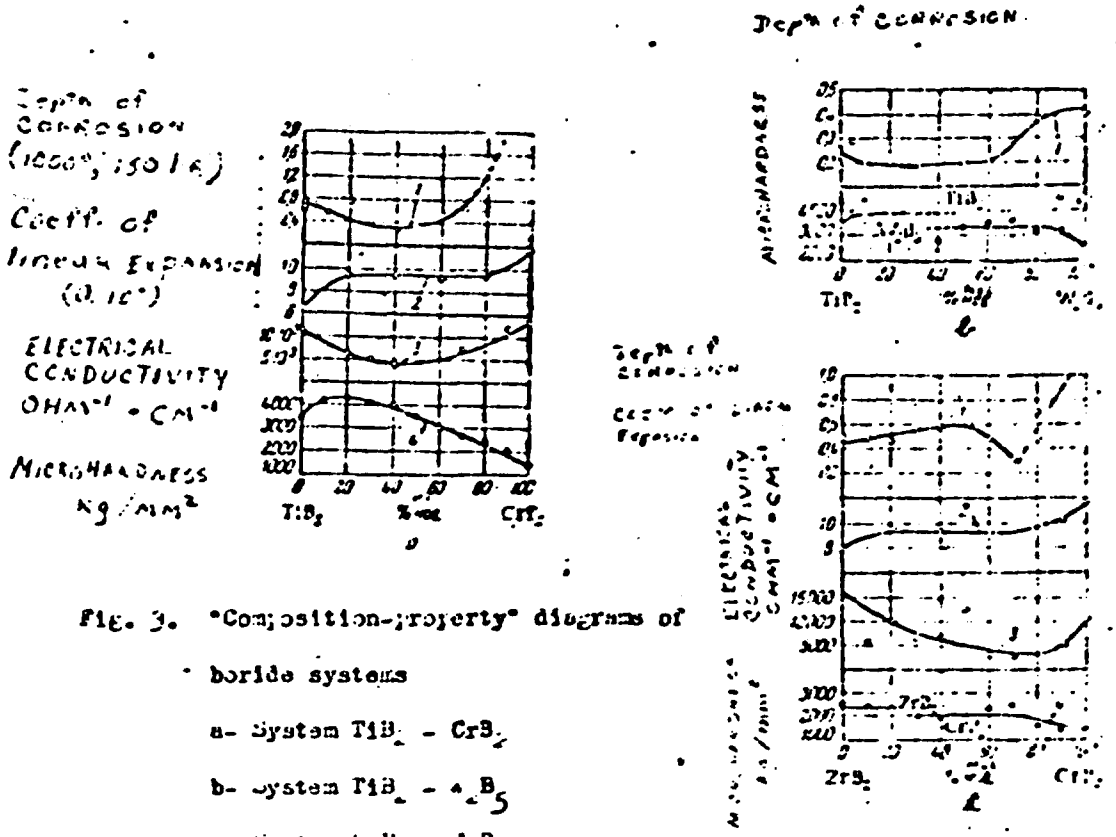

Fig. 3. "Composition-property" diagrams of boride systems

a- System TiB_2 - CrB_2

b- System TiB_2 - Ta_2B_5

c- System ZrB_2 - CrB_2

1. Depth of corrosion; 2. Coefficient of linear expansion;

3. Electrical conductivity; 4. Microhardness.

The thermal coefficient of linear expansion of alloy samples was measured in a temperature range of 20 to 700° by a quartz dilatometer [15]. The general view and diagram of the instrument are shown in Fig. 4.

The instrument consists of a horizontal tubular electric furnace (1) with a nichrome heater, in the center of which is a quartz tube (2). One end of the tube is soldered, and the other is fastened with clamps (3) to the table (4) of the microscope (11).

The test sample (5) (diam 8 mm, length 15 to 20 mm) is placed in a graphite holder (6) for centering and for a more uniform heating of the sample. By means of a flat steel spring (7) the sample is pressed by a quartz rod (9), which in turn abuts against the soldered end of the tube (2).

Spring (7) is fastened to tube (2) by clamps (10). The movement of rod (8) due to the pressure of sample (5) expanding during heating (or due to the pressure of spring (7) when compressed) is measured by a microscope (11) with an ocular micrometer gage (14) of the AM9-1 type. Readings are taken from indicator (12), which is a metal frame with an attached cover glass on which fine graduated lines are drawn.

The temperature is measured by a chromel-alumel thermocouple (13), the junction of which is placed in the side opening of the graphite holder (6) to a depth corresponding to the middle of the sample. It was established that at a temperature increase of about 5 to 6° per minute there was no noticeable drop in temperature between the sample and the thermocouple.

The results of the measurements are given in Fig. 5 (curves 2).

The limit of compressive strength was determined on a 12-ton manual hydraulic press by means of special equipment. Prismoid fragments of the alloy were compressed. The limit of bending strength was determined by means of

special equipment on a GZIP-5 testing machine. The cylindrical samples 14 mm in diameter and 3 to 4 mm high were bent through their diameter.

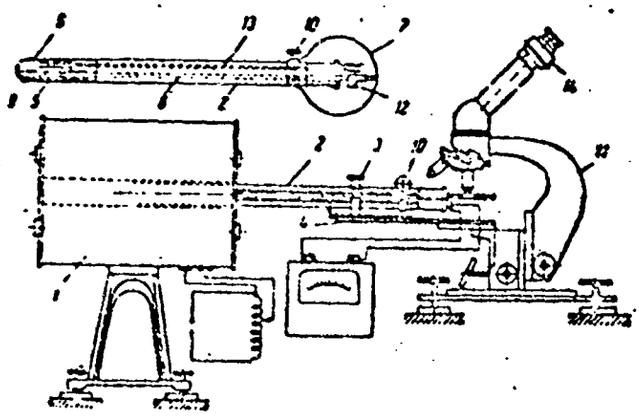

Fig. 4. Diagram of a quartz dilatometer installation

(1) Electric tubular furnace; (2) quartz test tube

(3) clamp for fastening test tube; (4) table for microscope;

(5) sample; (6) graphite holder; (7) compression spring;

(8, 9) quartz rods; (10) clamp to hold spring;

(11) microscope; (12) calibrated indicator; (13) thermocouple; (14) ocular micrometer gage.

Results of all measurements are given in Table 3. For comparison, data available in the literature are given in the Table.

On the basis of data from metallographic and x-ray diffraction analyses, and also from the results of measuring the microhardness of alloy phases and electrical conductivity (see Fig. 3), it can be concluded that in the system

TiB_2 - CrB_2 crystallization of a continous series of solid solutions occurred, but in systems TiB_2 - W_2B_5 and ZrB_2 - CrB_2 only limited solubility was observed. The solubility of TiB_2 in W_2B_5 and W_2B_5 in TiB_2 does not exceed 10 and 5% mole respectively. The solubility of ZrB_2 in CrB_2 is about 20% mole and the solubility of CrB_2 in ZrB_2 is evidently negligible.

TABLE 3

Properties of Boridos of Titanium, Zirconium, Curomium and Tungsten

(in brackets - published data)

Indices	TiB_2	ZrB_2	CrB_2	W_2B_5
Microhardness, Kg/mm^2	3 430±200	2 500±200	1 500±130	2 600±130
	(3 370)	(2 250)	(1 800)	(2 660)
Electrical conductivity *				
$ohm^{-1} cm^{-1}$	12 100±1 500	100 000	10 600	—
	(37 700)	(109 000)	(47 600)	—
Thermal coefficient of linear expansion, $\alpha . 10^6$	6.8	8.2	9.8	—
Ultimate strength kg/mm^2				
in compression	350	170	100	70
in bending	70	50	45	—

* Computed on the basis of 100% density

The study of corrosion resistance. The total oxidation process of borides can be expressed by equations:

$$MeB_n + \frac{1}{2}\left(m + \frac{3}{2}n\right)O_2 = MeO_m + \frac{n}{2}B_2O_3$$

According to published data the solubility of the oxides of titanium, zirconium, and chromium in B_2O_3 at temperatures below 1200° is small, and these metals do not form borates (in the present study this assumption was checked and confirmed). Thus, at the first moment of oxidation, at 1000° a mechanical mixture of B_2O_3 and the oxide of the corresponding metal is formed on the surface of the borides.

Having accepted the diffusion character of oxidation and considering the rate of evaporation of B_2O_3 as constant and equal to B, we obtain the following equation of the kinetics of boride oxidation (or of other chemical compounds in the oxidized scale of which there are volatile components):

$$\Delta G = At^{\cdot} - Bt \qquad (1)$$

where ΔG is change of weight per unit surface of the sample;

A is the constant of oxidation rate;

B is the evaporation rate of B_2O_3 per unit surface;

t is the time of oxidation.

Since the oxidation rate decreases with time and the evaporation rate of B_2O_3 can be taken as constant, there will arrive a moment when the evaporation rate will become equal to the oxidation rate and then will exceed it. Therefore, after a certain period of time, almost all the B_2O_3 in the scale will be evaporated. From that moment the scale will consist mostly of metal oxide.

and the process of oxidation will be described by a parabolic dependence:

$$\Delta G = A_1 t^{0.5} \qquad (2)$$

where $A_1 < A$

It follows from this that the oxidation process of borides can be divided into two stages. The kinetic curves of boride oxidation will divide correspondingly into two sectors.

Analysis of Eq. (1) leads to a series of dependences.

The duration of the first stage of oxidation:

$$t_1 = \left(\frac{A - A_1}{B}\right)^2 \quad \text{OR} \quad t_1 = \left[\frac{A}{B}(1 - K_1)\right]^2 \qquad (3)$$

where K_1 is the coefficient, showing which portion of the increase in weight is due to the formation of metal oxides.

The value of K_1 is determined only by stoichiometric ratios (see the general equation for the reaction of boride oxidation:

$$K_1 = \frac{m}{m + \frac{3}{2}n} \qquad (4)$$

If $K_1 < 0.5$, then during a certain period of time the weight of the sample will decrease in the process of oxidation; i.e. the maximum will appear on the sector of curve ΔG -t corresponding to the first stage of oxidation. To this maximum corresponds the time:

$$t_1 = \left(\frac{A}{2B}\right)^2 \qquad (5)$$

The period of time $t_2 - t_1$, during which oxidation is accompanied by a decrease in weight, is:

$$t_2 - t_1 = \left[\frac{A}{B}\right]^2 (0.5 - K_1)(1.5 - K_1) \qquad (6)$$

In order to determine the coefficients A and B in Eq. (1), it is necessary to plot an experimental curve in coordinates ΔG and $\sqrt{t}$, where

$$z = \frac{\Delta G}{t} \qquad (7)$$

The angle of slope of the straight line will equal A; the intercept on the axis will correspond to B.

In general the process of oxidation can be described not by a parabolic, but by a step dependence and Eq. (1) will have the form:

$$\Delta G = At^{n} - B \qquad (8)$$

The curve described by Eq. (8) is rectified when plotting in coordinates log (z B) and log t.

The change in weight of the sample (weight-increase), which is fixed by various weighting methods of testing (without removing the scales), and the change in the outer dimensions of the sample cannot uniquely characterize the oxidation resistance of the material.

Depth corrosion is an indicator comparable for different materials and uniquely characterizing the degree of corrosion and, therefore, the corrosion resistance.

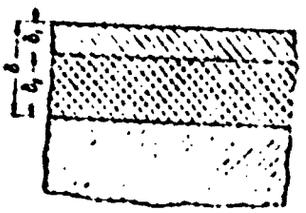

Fig. 5. Diagram of the scale formation.

By examining the dependence between the change in weight (ΔG), the

depth of corrosion (δ_1) and the change in outer dimensions of the sample (δ_1) in the process of oxidizing (Fig. 5), the following relations can be derived:

$$\delta_1 = K_2 \Delta G \tag{9}$$

$$\delta_1 = K_3 \Delta G \tag{10}$$

$$\delta = \delta_1 + \delta_1 = (K_2 + K_3)\Delta G \tag{11}$$

where δ_1 is the depth of corrosion,

δ_1 is the change of outer dimensions of sample due to corrosion, μ;

the scale thickness, μ;

K_2 is the coefficient-equal to the depth of corrosion (in μ)

during the change in the weight of the sample by 1 mg/cm^2

K_3 is the coefficient equal to the change in the outer dimensions of sample (in μ) during the change in the weight of the sample by 1 mg/cm^2.

Values K_2 and K_3 can be calculated by formulas:

$$K_2 = \frac{10}{\gamma_c \left(\frac{M_{ox}}{M_c} - 1 \right)} \qquad K_3 = K_2(\alpha - 1) \tag{12}$$

where γ_c is the specific weight of the oxidizing compound

M_c is the molecular weight of the oxidizing compound

M_{ox} is the weight of the oxides formed by oxidation of 1 mole of the compound.

α is the Pilling-Bedworth ratio (volume of oxidation: volume of compound).

Table 4 shows coefficient values of α, K_2, K_3 and K_3 for TiB_2, ZrB_2, CrB_2 and VB_2. For comparison, data is given for some other compounds and alloys.

TABLE 4

Coefficients α, K_1, K_2, and K_3 For

Certain Compounds and Alloys

Material	α Allowing for the B_2O_3	α Without allowing for the B_2O_3	K_1	K_2	K_3
TiB_2	3.70	1.36	0.40	14.8	5.3
ZrB_2	3.21	1.22	0.40	7.8	3.9
CrB_2	3.73	1.04	0.50	6.0	2.5
W_2B_5	2.95	2.00	0.44	7.7	7.7
TiC	—	1.54	—	6.1	3.3
TiC+20% Co	—	1.60	—	6.1	3.3
Fe	—	2.17	—	2.9	3.4
$MoSi_2$	—	2.95	—	2.2	4.1
SiAl	—	1.45	—	3.4	1.5
SiC	—	1.84	—	7.5	3.8
67% SiC+33% B_4C	—	1.17	—	∞	∞

Note: When calculating it was understood that the scales consisted of oxides of TiO_2, ZrO_2, Cr_2O_3, MoO_3, CoO, Fe_2O_3, Al_2O_3, SiO_2.

Oxidation Rate of Boride and Their Alloys

In order to study the oxidation rate during a protected period (up to 170 hours), a gravimetric method was used with periodical removing of samples

from the furnace for weighing and measuring. To study the initial oxidation period (2 to 4 hours), the method of periodic weighing was used without removing the samples from the furnace. The samples, placed on porcelain disks, were loaded into a muffle furnace (Fig. 6). Oxidation occurred at 1000°.

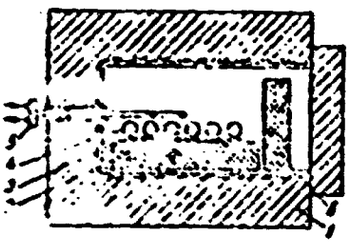

Fig. 6. Diagram of loading samples in the furnace when studying the kinetics of oxidation:
1- muffle; 2- refractory brick; 3- porcelain disks;
4- samples; 5- thermocouple; 6- refractory shield.

The kinetic curves of oxidation for certain samples are given in Fig. 7.

Mathematical processing of the experimental data by the above method showed that the oxidation process in all cases can be satisfactorily described by Eq. (3). The value of the exponent n equals 0.5 within the limits of accuracy of the test.

As an example, data are given in Table 5 on the oxidation rate of TiB_2 samples.

The oxidation rate of zirconium diboride and its alloys with a small quantity of TiB_2 and ZrB_2 is of interest. During short exposures, zirconium diboride, and particularly its alloys containing 10 to 20 mole % of TiB_2 and ZrB_2, remains in weight very slightly. However, during longer oxidation

(longer than 20 to 30 hours) the weight increase of the samples rose sharply (tens of times).

TABLE 5

Oxidation Rate TiB_2

Time of oxidation, hrs.	Weight increase		Change in outer dimensions		Calculated depth of corrosion
	Experimental	Calculated	Experimental	Calculated	
0.8	6.8	5.2	0.025	0.036	0.10
2.8	10	9.2	0.045	0.055	0.15
9.3	19	15	0.080	0.10	0.28
19	25	20	0.090	0.13	0.37
29	20	23	0.135	0.16	0.45
40	24	26	0.165	0.18	0.52
48	28	28	—	0.20	0.56
63	29	29	0.18	0.21	0.58
82.5	32	29	0.17	0.22	0.62
102	30	30	0.185	0.21	0.59
119	29	29	—	0.21	0.58
147	29	29	0.19	0.21	0.58
170	31	31	0.33	0.22	0.61

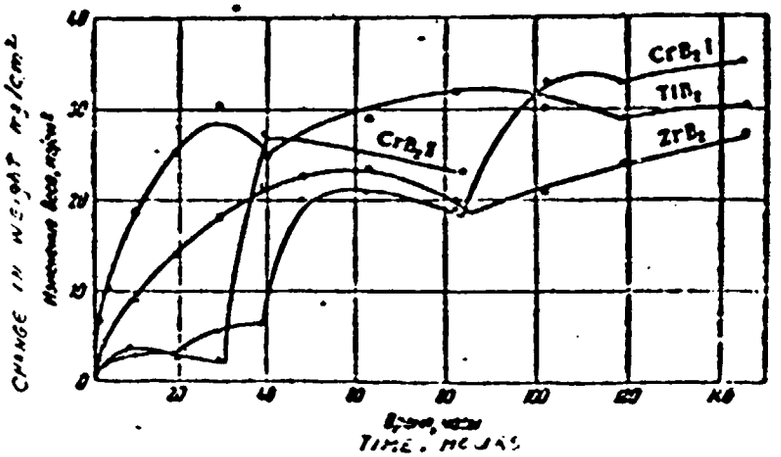

Fig. 7. Kinetic curves of oxidation of samples (in a muffle furnace, in air atmosphere, and at 1000°).

Several similar jumps could be observed on the kinetic curves of oxidation of pure CrB_2 (Fig. 7). The reason for such abrupt deterioration of the protective qualities of the scale is its insufficient stability, due evidently to the very small values of coefficient α (the ratio of the volume of the forming scale to the volume of the oxidized material, see Table 4).

The data on the weight increase and depth of corrosion, calculated by formula (4) and obtained during oxidation of various alloys, for 150 hours at 1000°, are given in Table 6 and in Fig. 3 (curves 1).

As can be seen in Fig. 3,a, the depth of corrosion of the intermediate alloys in the TiB_2 - CrB_2 system is considerably less than for the pure components. The scale on these intermediate samples differed sharply from the scale on TiB_2 and CrB_2. It can be assumed that in the present case the formation of a chemical compound of TiO_2 and Cr_2O_3 takes place and this compound has the high protective properties characteristic of Cr_2O_3, and at a favorable value of α, characteristic also of TiB_2. Such a chemical compound $Cr_2O_3 \cdot TiO_2$, which probably has an orthorhombic lattice, was discovered

by McBride and his collagues 16 .

TABLE 6

Weight change ΔG (in mg/cm^2) and depth of corrosion δ_l (in mm) during oxidation of borides and their alloys in the air at 1000° for 150 hours

(in brackets - extrapolated data)

Composition, % mole		$TiB_2 - CrB_2$		$TiB_2 - W_2B_5$		$ZrB_2 - CrB_2$	
A	B						
100	0	29	0,48	29	0,58	30	0,54
90	10	60	0,94	16	0,19	24	0,45
80	20	41	0,63	23	0,23	38	0,76
70	30	—	—	19	0,18	25	0,56
60	40	11	0,26	31	0,29	23	0,57
50	50	12	0,32	26	0,23	22	0,60
40	60	18	0,54	34	0,29	15	0,45
30	70	20	0,68	—	—	(9)	(0,30)
20	80	37	1,3	47	0,39	—	—
10	90	—	1,7	—	—	(12)	(0,6)
0	100	35	2,1	44	0,33	35	2,1

* Oxidation during 50 hours.

3

In the system ZrB_2 - CrB_2 the dependence of the depth of corrosion on the composition is of a complex nature. With an increase in CrB_2 content to 40 to 50% mole, the depth of the corrosion increases somewhat; between 40 to 70% mole it decreases and then again rises sharply.

The corrosion resistance of the investigated borides increases in the following order: W_2B_5 - TiB_2 - ZrB_2 - CrB_2 (at small exposures). The corrosion resistance of TiB_2, ZrB_2, CrB_2, and particularly their alloys, exceeds the corrosion resistance of titanium carbide, but is lower than that of some silicides. The corrosion resistance of the borides, which is lower by comparison with the silicides, is evidently due to the substantial difference between SiO_2 and B_2O_3. The film of boron oxide formed by the oxidation of the borides cannot serve effectively as a protection against oxidation, because of low viscosity and high volatility, and the protective properties of the boride scales are primarily determined by the properties of the metal oxides.

The fact that the corrosion resistance of borides is higher than the resistance of the corresponding carbides, and even more so of the metals, shows however that the presence of boron oxide in the products of oxidation substantially increases corrosion resistance. It is evident that with any oxidation time the content of B_2O_3 in the inner layers of the scale is considerable, whereas in the outer layers B_2O_3 is practically non-existant. When therefore the borides are oxidized, there occurs continuous diffusion of the molten B_2O_3 through the layer of the scale and its subsequent evaporation from the surface. As a result of a certain (though insignificant) mutual solubility of B_2O_3 and MeO, the presence of B_2O_3 in the scale accelerates the oxidation of the borides at high oxidation temperatures (owing to the presence of a liquid phase). In the oxidation of carbides and nitrides

3

the escaping gases (CO, CO_2, N_2) react in the opposite way; they loosen the scale.

Thus it may be presumed that, during oxidation of borides, a process of "self-healing" of the scale occurs, although to a lesser degree than with silicides [17]. Upon the appearance of a small crack or some other defect in the scale, an intensive oxidation of the boride begins; the products of oxidation (MeO & B_2O_3), which occupy a large volume, quickly fill the crack, thus preventing the access of oxygen. After that, the greater part of the boron oxide evaporates, leaving a dense layer of metal oxide "welding" the crack.

Scale Structure. The study of the scale structure was made on prepared sections of the scale and also on oblique sections. In some cases, the samples were drenched with polymethylmetacrylate. The change in the outer appearance of the samples during oxidation confirms the assumption that first a mechanical mixture of metal oxides and B_2O_3 forms. After a while, the B_2O_3 content in the outer layers of the scale becomes negligible. In alloys TiB_2 - Ti_2B_5 and ZrB_2 - CrB_2 there evidently forms a mechanical mixture of oxides of the corresponding metals. In alloys TiB_2 - CrB_2 the character of the scale differs considerably from the TiB_2 and CrB_2 scale.

The study of the oblique sections and the prepared sections of the scale showed that in most cases multilayered scales form, the inner layers of which consist of lower oxides (TiO, Ti_2O_3, Cr_2O_3). The presence of comparatively thick layers of these oxides in the scale of the borides testifies to the decreased partial oxygen pressure in the inner layers of the scale.

It is interesting to examine from this point of view the results of oxidation of zirconium boride. With an increase in oxidation time, the

3

color of the surface of the sample changes from bluish-black through dull-black and grey to grey-white. Simultaneously, the surface character changes from a very smooth, glossy ("lacquered") surface to a dull one. In studying the cross and oblique cuts of the scale (Fig. 8) and the prepared sections, a black layer clearly appears between the boride base and the thick white layer of ZrO_2. All these facts can be explained by the formation of lower oxides of zirconium, probably ZrO, the existence of which has been denied in the majority of studies [18, 19]. However, the conclusion regarding the existence of ZrO (and Zr_2O_3) was confirmed by chemical and x-ray diffraction analyses in subsequent studies [20]. The data obtained in the present work also confirm the presence of lower zirconium oxides.

Fig. 8. Scale on zirconium boride

(A) Boride base; (B) thin black layers of lower oxides (probably ZrO); (C) layer of ZrO_2.

Thus it can be assumed that oxidation of zirconium boride at 100° occurs in the following way. In the initial period (1 to 2 hours) a film forms on the surface of the boride of ZrO which is covered by a layer of semi liquid boron oxide or having a solution of ZrO in it. In the course of the next 10 to 20 hours, as a result of diffusion of oxygen, ZrO is oxidized to ZrO_2. Judging by the outer appearance of the scale at this stage of oxidation, it can be assumed that oxidation of ZrO occur along the entire thickness of the vitreous layer of boron oxide and the forming particles of ZrO_2 form a similar supension in B_2O_3. Upon further oxidation, the boron oxide gradually evaporates and on the surface of the sample of ZrO_2 it gradually forms a scale. The inner layers of ZrO_2 are very dense and hard, and therefore the ZrO layer retains a considerable thickness.

References

1. Shaler, A., Hoffman, J.: Inst. Met., 8.8 (1954).
2. Aeron. Age, 173, No. 13, 138 (1954).
3. Evernert, I.: Materials a. methods, 40, 90 (1954).
4. Steinitz, R., Binder, I.: Powder Met Bull., 6, 123 (1953).
5. Kornilov, I. I.: DAN SSSR, 81, 597 (1951).
6. Post, B., Glaser, F. W.: J. Chem. Phys., 20, 1050 (1952).
7. Umanskiy, Ya. S.: Carbides of Hard Alloys (Karbidy tverdykh splavov): Metallurgizdat, (1947).
8. Umanskiy, Ya. S., Finkelstein, B. N., Blanter, M. E., Kishkin, S. T., Fastov, N. S., Gorelik, S. S.: Physical Metallurgy (Fizicheskoye Metallovedeniye), (1955).

3